



ELSEVIER

Available online at www.sciencedirect.com

SCIENCE @ DIRECT®

Journal of Sound and Vibration 280 (2005) 467–478

JOURNAL OF
SOUND AND
VIBRATION

www.elsevier.com/locate/jjsvi

Transverse vibration and stability of an eccentric rotating circular plate

Ratko Maretic*

Faculty of Technical Sciences, University of Novi Sad, P.O. Box 55, 21121 Novi Sad, Serbia and Montenegro

Received 21 July 2003; accepted 24 November 2003

Available online 2 September 2004

Abstract

A thin circular plate rotating at constant angular speed around the axis perpendicular to the plane of the plate is investigated in this paper. The axis of rotation is parallel to the plate's axis of symmetry and the distance between them is the plate's eccentricity. The outer edge of the plate is attached to a rigid body rotating together with the plate. The stresses and displacements in the plate's middle plane are determined in the paper. The natural frequencies of the transverse vibration with respect to angular speed and eccentricity are determined using Galerkin's method. The mode shapes for the certain frequencies are shown. Due to the plate's eccentricity and rotation, the mode shapes are deformed in comparison with the plate without eccentricity. It is shown that frequencies split for the asymmetric mode shapes, so that there are two different frequencies in those cases. The critical angular speed which results in stability loss in the first mode is determined.

© 2004 Elsevier Ltd. All rights reserved.

1. Introduction

Rotating plates are often parts of mechanical structures, which led to their being intensively investigated during the recent years. Numerous examples show that ideal rotation is assumed when conducting these investigations. However, manufacturing and mounting of a plate usually result in the imperfect alignment, i.e. the misalignment between the axis of rotation and the axis of

*Tel.: +381-21-350-122x117; fax: +381-21-58-133.

E-mail address: maretic@uns.ns.ac.yu (R. Maretic).

symmetry. As a result of this, the plate rotates eccentrically. This phenomenon can influence the stresses and vibration of such a plate.

In certain devices eccentric rotating plates and discs are intentionally used. These devices are applied in centrifuges, separators, rheometers, pumps, mechanical spectrometers, in the vacuum technology, etc.

There is a great number of papers which have investigated eccentricity of annular plates and discs. Mitchell and Warren [1] have determined the stress and displacement fields in a thin circular disc rotating at the constant angular speed around an eccentric rigid insert. Lurie [2] has determined the stresses in a rotating circular disc. These papers show that eccentricity of the plate's rotation greatly influences the stresses and displacements in the plate's plane.

Various examples of the impact of the plate's asymmetry on the frequency of the transverse vibrations can be found among published works. For example, Khurasia and Rewtant [3] have examined the effect of the existence of an eccentric hole on the circular plate on its vibration. It has been shown that eccentricity of the central hole results in a significant change in frequencies and mode shapes. A similar problem has been theoretically and experimentally investigated by Cheng et al. [4]. It has been pointed out that the existence of an eccentricity will lead to the splitting the frequency and making it double with a corresponding impact on the vibration mode.

Parker and Mote [5] have proposed a method for predicting natural frequencies of stationary annular and circular plates with a slight deviation from axisymmetry. They have also discussed the phenomenon of natural frequencies splitting.

Some authors have also examined rotating discs where the axis of rotation is misaligned with the axis of symmetry. Chung et al. [6] have studied the effects of misalignment on the natural frequencies of a rotating disc using Galerkin's method. They have pointed out the existence of the critical angular speed, among other things. Heo et al. [7] have analysed dynamic time response of a misaligned rotating disc using the finite element method.

These papers have mostly investigated annular plates and discs with an imperfection of shape or rotation. However, there are also cases of imperfection of rotating circular plates. Fig. 1 shows examples of such plates. A plate of radius R and thickness h is clamped on the outer edge to a rigid body of a suitable shape rotating together with the plate at a constant angular speed ω . They rotate together around the axis c , while o denotes the axis of symmetry of the plate. The eccentricity of the plate, i.e. the distance between the axes o and c , is d . The support, which is not shown, prevents the rigid body from moving in the radial direction, as well as in the direction perpendicular to the plate's plane. The bottoms of rotating vessels and centrifuges where eccentricity is present and walls, which can be considered to be rigid compared to the bottom can

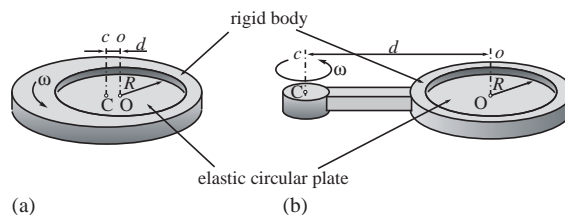


Fig. 1. The examples of an eccentric rotating circular plate: (a) $d < R$; (b) $d > R$.

be modelled in this way. The case shown in Fig. 1b can be observed in lids of openings for cleaning and intervention on large rotating vessels in industry.

The impact of angular speed and eccentricity on transverse vibration frequencies of the circular plate shown will be examined in this paper. The mode shapes will be studied, the conditions leading to the plate’s stability loss will be checked and the corresponding critical parameters will be determined. It will also be shown that some shape modes result in frequency split.

2. Mathematical formulation of the problem

Consider a circular plate shown in Fig. 2 with the centre at point O rotating around an axis perpendicular to the plane of the plate at point C . Let (r, θ, z) be a movable cylindrical coordinate system fixed to the middle plane of the plate with the origin at the centre of the plate O and the axis z perpendicular to the plate. The unit vectors \mathbf{r}_0 and \mathbf{c}_0 rotate together with the plate. The angle θ is measured starting at the line OC which is moving together with the plate, \mathbf{q} denotes the inertial force per unit area in the middle plane of the plate and it is given by

$$\mathbf{q} = (\mathbf{d} + r\mathbf{r}_0)\rho h\omega^2, \tag{1}$$

where ρ denotes the mass per unit volume.

The components of the inertial force along the radial and circumferential axes are

$$q_r = \rho h\omega^2(r + d \cos \theta), \quad q_c = -\rho h\omega^2 d \sin \theta \tag{2}$$

The force–displacements relationships in the polar coordinate system are

$$N_r = \frac{Eh}{1 - \nu^2} \left[\frac{\partial u}{\partial r} + \nu \left(\frac{1}{r} \frac{\partial v}{\partial \theta} + \frac{u}{r} \right) \right], \tag{3}$$

$$N_c = \frac{Eh}{1 - \nu^2} \left[\frac{1}{r} \frac{\partial v}{\partial \theta} + \frac{u}{r} + \nu \frac{\partial u}{\partial r} \right], \tag{4}$$

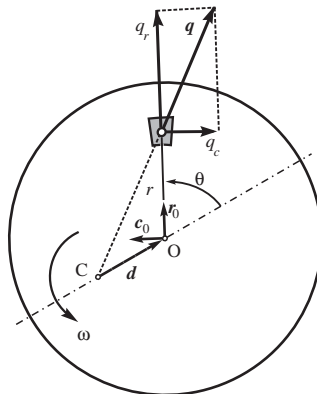


Fig. 2. Geometry, load and coordinates of the plate.

$$N_{rc} = \frac{Eh}{2(1+\nu)} \left[\frac{1}{r} \frac{\partial u}{\partial \theta} + \frac{\partial v}{\partial r} - \frac{v}{r} \right], \quad (5)$$

where N_r and N_c are normal in-plane forces, and N_{rc} is a shear force, u and v denote the radial and circumferential displacements of the middle plane, E denotes Young's modulus and ν Poisson's ratio.

The normal forces and the shear force in the plate are given by the equations of equilibrium

$$\frac{\partial}{\partial r}(rN_r) - N_c + \frac{\partial N_{rc}}{\partial \theta} + rq_r = 0, \quad (6)$$

$$\frac{\partial N_c}{\partial \theta} + \frac{\partial}{\partial r}(rN_{rc}) + N_{rc} + rq_c = 0. \quad (7)$$

The transverse motion of the plate is modelled using the classical Kirchhoff plate theory with in-plane stresses. The governing differential equation of the motion is

$$\begin{aligned} D\nabla^4 w = & -h\rho \frac{\partial^2 w}{\partial t^2} + N_r \frac{\partial^2 w}{\partial r^2} + N_c \left(\frac{1}{r} \frac{\partial w}{\partial r} + \frac{1}{r^2} \frac{\partial^2 w}{\partial \theta^2} \right) \\ & + 2N_{rc} \frac{\partial}{\partial r} \left(\frac{1}{r} \frac{\partial w}{\partial \theta} \right) - q_r \frac{\partial w}{\partial r} - q_c \frac{1}{r} \frac{\partial w}{\partial \theta}, \end{aligned} \quad (8)$$

where w denotes the transverse displacement of the plate and $D = Eh^3/12(1-\nu^2)$ is the flexural rigidity.

The boundary conditions are given by

$$u|_{r=R} = 0, \quad v|_{r=R} = 0, \quad w|_{r=R} = 0, \quad \left. \frac{\partial w}{\partial r} \right|_{r=R} = 0. \quad (9)$$

Substituting Eqs. (2)–(5) into Eqs. (6) and (7) and solving them with respect to the boundary conditions yields

$$u = \frac{\rho\omega^2}{E} (1-\nu^2)(R^2 - r^2) \left(\frac{r}{8} + \frac{d}{3-\nu} \cos \theta \right), \quad (10)$$

$$v = -\frac{\rho\omega^2}{E} \frac{1-\nu^2}{3-\nu} (R^2 - r^2) d \sin \theta. \quad (11)$$

Substituting Eqs. (10) and (11) into Eqs. (3)–(5) results in

$$N_r = \rho\omega^2 h \left(\frac{1+\nu}{8} R^2 - \frac{3+\nu}{8} r^2 - \frac{2d}{3-\nu} r \cos \theta \right), \quad (12)$$

$$N_c = \rho\omega^2 h \left(\frac{1+\nu}{8} R^2 - \frac{1+3\nu}{8} r^2 - \frac{2vd}{3-\nu} r \cos \theta \right), \quad (13)$$

$$N_{rc} = \rho\omega^2 h d \frac{1-\nu}{3-\nu} r \sin \theta. \quad (14)$$

Based on the Eqs. (12)–(14) the normal and tangential stresses in the middle plane of the plate can be determined. Substituting Eqs. (2), (12)–(14) into Eq. (8) using the nondimensional expressions

$$y = \frac{w}{h}, \quad x = \frac{r}{R}, \quad \tau = t \sqrt{\frac{D}{h\rho R^4}}, \quad \lambda = \frac{\rho\omega^2 R^4}{Eh^2}, \quad e = \frac{d}{R} \tag{15}$$

gives

$$\begin{aligned} \nabla^4 y - \eta \left[(N_1 + N_2 \cos \theta) \frac{\partial^2 y}{\partial x^2} + (C_1 + C_2 \cos \theta) \left(\frac{1}{x} \frac{\partial y}{\partial x} + \frac{1}{x^2} \frac{\partial^2 y}{\partial \theta^2} \right) \right. \\ \left. + 2S_1 \sin \theta \left(\frac{1}{x} \frac{\partial^2 y}{\partial x \partial \theta} - \frac{1}{x^2} \frac{\partial y}{\partial \theta} \right) - \lambda(x + e \cos \theta) \frac{\partial y}{\partial x} + \frac{\lambda e}{x} \frac{\partial y}{\partial \theta} \sin \theta \right] + \frac{\partial^2 y}{\partial \tau^2} = 0, \end{aligned} \tag{16}$$

where

$$\begin{aligned} N_1 &= \frac{\lambda}{8} [1 + \nu - (3 + \nu)x^2], & N_2 &= -\frac{2\lambda ex}{3 - \nu}, \\ C_1 &= \frac{\lambda}{8} [1 + \nu - (1 + 3\nu)x^2], & C_2 &= -\frac{2\lambda ex\nu}{3 - \nu}, \\ S_1 &= \frac{1 - \nu}{3 - \nu} \lambda ex, & \eta &= 12(1 - \nu^2). \end{aligned} \tag{17}$$

The third and fourth boundary conditions in Eq. (9) are transformed into

$$y|_{x=1} = 0, \quad \left. \frac{\partial y}{\partial x} \right|_{x=1} = 0. \tag{18}$$

The problem of determining the transverse vibration frequency of an eccentric rotating plate is reduced to solving Eq. (16) respecting the boundary conditions given in Eq. (18).

3. Numerical solutions

The solution of Eq. (16) is obtained applying the Galerkin’s method. To this end, the solution is assumed in the form

$$\bar{y} = \left[\sum_{m=0}^M A_{m0} Y_{m0}(x) + \sum_{m=0}^M \sum_{n=1}^N (A_{mn} \cos n\theta + B_{mn} \sin n\theta) Y_{mn}(x) \right] \sin \Omega\tau, \tag{19}$$

where A_{mn} and B_{mn} are undetermined coefficients, and M and N are the numbers of the basic functions used in the approximation.

The nondimensional natural frequency Ω of the transverse vibration is

$$\Omega = \Omega_N \sqrt{\frac{\rho h R^4}{D}}, \tag{20}$$

where Ω_N is the natural frequency. Y_{mn} are the functions chosen to satisfy the boundary conditions of the plate. They are presently assumed to be of the following form:

$$Y_{mn} = (1 - x^2)^2 x^{2m+n}. \tag{21}$$

Substituting Eqs. (19) and (21) into Eq. (16) and applying the Galerkin’s procedure the following equations are obtained

$$\sum_{m=0}^M [2A_{m0}(\alpha_{m0i0} - \Omega^2 \zeta_{m0i0}) + A_{m1}(\beta_{m1i0} - \zeta_{m1i0})] = 0, \quad i = 0, 1, \dots, M, \tag{22}$$

$$\begin{aligned} & \sum_{m=0}^M 2A_{m0} \beta_{m0ij} \delta_{1j} \\ & + \sum_{m=0}^M \sum_{n=1}^N A_{mn} [2(\alpha_{mnij} - \Omega^2 \zeta_{mnij}) \delta_{nj} + \beta_{mnij}(\delta_{na} + \delta_{nb}) + \zeta_{mnij}(\delta_{na} - \delta_{nb})] = 0, \\ & i = 0, 1, \dots, M, \quad j = 1, \dots, N, \end{aligned} \tag{23}$$

$$\begin{aligned} & \sum_{m=0}^M \sum_{n=1}^N B_{mn} [2(\alpha_{mnij} - \Omega^2 \zeta_{mnij}) \delta_{nj} + \beta_{mnij}(\delta_{na} + \delta_{nb}) + \zeta_{mnij}(\delta_{na} - \delta_{nb})] = 0, \\ & i = 0, 1, \dots, M, \quad j = 1, \dots, N, \end{aligned} \tag{24}$$

where $a = j - 1$ and $b = j + 1$, while

$$\begin{aligned} \delta_{ks} &= \begin{cases} 0 & \text{for } k \neq s, \\ 1 & \text{for } k = s, \end{cases} \\ \alpha_{mnij} &= \int_0^1 a_{mn} Y_{ijx} dx, \quad \beta_{mnij} = \int_0^1 b_{mn} Y_{ijx} dx, \\ \zeta_{mnij} &= \int_0^1 c_{mn} Y_{ijx} dx, \quad \xi_{mnij} = \int_0^1 Y_{mn} Y_{ijx} dx. \end{aligned} \tag{25}$$

The expressions to be integrated in Eq. (25) are

$$\begin{aligned} a_{mn} &= \frac{d^4 Y_{mn}}{dx^4} + \frac{2 d^3 Y_{mn}}{x dx^3} - \left[\frac{1 + 2n^2}{x^2} + \eta N_1 \right] \frac{d^2 Y_{mn}}{dx^2} \\ &+ \left[\frac{1 + 2n^2}{x^3} - \frac{\eta}{x} C_1 + \eta \lambda x \right] \frac{d Y_{mn}}{dx} \\ &+ \left[\frac{n^4 - 4n^2}{x^4} + \eta C_1 \frac{n^2}{x^2} \right] Y_{mn}, \end{aligned}$$

$$\begin{aligned}
 b_{mn} &= \eta \left[-N_2 \frac{d^2 Y_{mn}}{dx^2} + \left(\lambda e - \frac{C_2}{x} \right) \frac{d Y_{mn}}{dx} + C_2 \frac{n^2}{x^2} Y_{mn} \right], \\
 c_{mn} &= -\eta \frac{n}{x} \left(2S_1 \frac{d Y_{mn}}{dx} - \frac{2}{x} S_1 Y_{mn} + \lambda e Y_{mn} \right).
 \end{aligned}
 \tag{26}$$

Two independent equation systems have been formed in this way. The first consists of Eqs. (22) and (23) and is used to determine the A_{mn} coefficients. The second contains Eq. (24) and is used to determine the B_{mn} coefficients. Based on these equation systems two frequency equations are formed.

When $\lambda = 0$ or $e = 0$ solving Eqs. (22) and (23) provides symmetric and asymmetric solutions, and when solving Eq. (24) only asymmetric solutions are obtained, which are the same in both cases. However, if $\lambda > 0$ and $e > 0$, the solutions of the formed frequency equations are different. That means that in the same mode shapes the frequency split occurs. The frequency split occurs in the case of asymmetric modes ($n \neq 0$), so the frequencies obtained from Eqs. (22) and (23) will be denoted by the index c (because the A_{mn} coefficients multiply $\cos n\theta$), for example $(0,1)_c$, while the frequencies obtained from Eq. (24) will be denoted by the index s (because the B_{mn} coefficients multiply $\sin n\theta$), for example $(0,1)_s$.

4. Results and discussion

The accuracy of the solutions obtained solving the frequency equations depends on the number of Y_{mn} functions used, and thus on the numbers M and N . The convergence test is shown in the Table 1, where the nondimensional frequencies Ω obtained for different mode shapes and different M and N values are compared. The mode (m,n) represents a mode with m nodal circles and n nodal diameters.

Table 1
Convergence characteristics of the frequencies parameter Ω

	M	N	Mode (m,n)						
			$(0,0)$	$(0,1)_c$	$(0,1)_s$	$(0,2)_c$	$(0,2)_s$	$(1,0)$	
$\lambda = 0$	2	2	10.21583	21.26047	21.26047	34.87767	34.877671	39.92111	
$e = 0$	3	3	10.21583	21.26040	21.26040	34.87704	34.877039	39.77330	
	4	3	10.21583	21.26040	21.26040	34.87703	34.877035	39.77116	
	4	4	10.21583	21.26040	21.26040	34.87703	34.877035	39.77116	
	5	4	10.21583	21.26040	21.26040	34.87703	34.877035	39.77115	
	Leissa [8]		10.216	21.261	21.261	34.877	34.877	39.771	
$\lambda = 10$	2	2	8.52412	21.59754	21.89370	36.34802	36.34854	41.22388	
	$e = 0.5$	3	3	8.51921	21.57181	21.87311	35.76150	35.76478	41.21033
		4	3	8.51867	21.57104	21.87304	35.76120	35.76465	41.20753
		4	4	8.51866	21.57082	21.87282	35.74801	35.75145	41.20752
		5	4	8.51865	21.57082	21.87282	35.74801	35.75144	41.20751

In this example, as well as in all others, the value of the Poisson ratio ν is assumed to be 0.3. The results obtained are compared with numerical results presented by Leissa [8].

Note that for $M > 3$ and $N > 3$ the vibration frequency changes insignificantly. The differences are bigger in the case of higher values of the nondimensional angular speed λ and nondimensional eccentricity e , as well as mode shapes. This paper assumes the values of $M = 5$ and $N = 4$.

Fig. 3 illustrates the changes in the nondimensional frequency Ω with respect to nondimensional angular speed λ and nondimensional eccentricity e in the fundamental mode shape (0,0). It can be seen that the increase in the angular speed and eccentricity leads to the decrease in the frequency of transverse vibration. All these functions show a monotonous decrease. Naturally, all the curves originate from the same point which represents the frequency of a stationary (not rotating) plate. The critical values of the angular speed can be discussed based on this figure. The critical angular speed is defined as the angular speed at which the natural frequency becomes zero. Table 2 shows

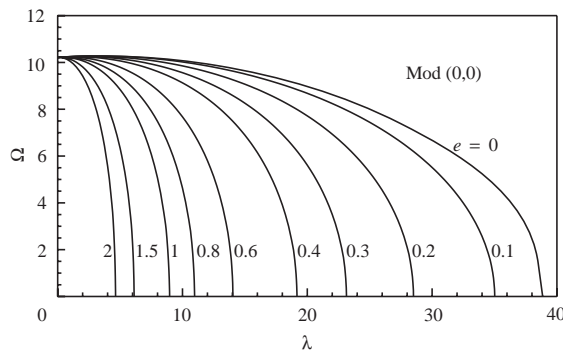


Fig. 3. The dependency of the nondimensional frequency Ω on the angular speed λ and nondimensional eccentricity e in the fundamental mode shape.

Table 2

The critical value of the nondimensional angular speed λ with respect to the eccentricity e

e	λ	Maretic [9]
0	38.8534	38.8533
0.1	35.0105	
0.2	28.5053	
0.3	23.1388	
0.4	19.1749	
0.5	16.2482	
0.6	14.0388	
0.7	12.3280	
0.8	10.9719	
0.9	9.8744	
1	8.9702	
1.5	6.1264	
2	4.6388	

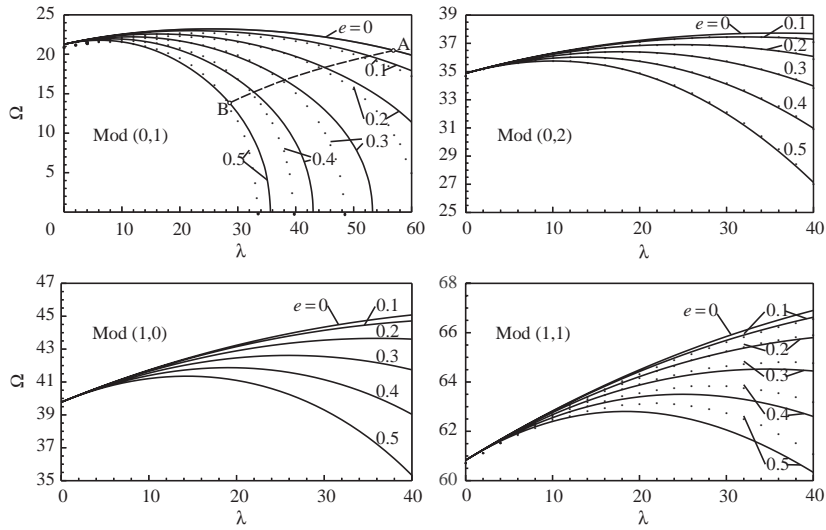


Fig. 4. The dependency of the nondimensional frequency Ω on the nondimensional angular speed λ and nondimensional eccentricity e : —, frequency c , ..., frequency s .

some critical values of the nondimensional angular speed with respect to eccentricity, as well as the comparison with the results given in the paper of Margetic [9]. It is obvious that the critical angular speed decreases monotonously when eccentricity increases.

Fig. 4 illustrates the changes in the nondimensional frequency Ω with respect to the parameter λ and eccentricity e for the modes shape (0,1), (0,2), (1,0) and (1,1). It can be noted here that the increase in eccentricity decreases the vibration frequency, similar to the fundamental mode shape case. However, these mode shapes in certain areas show the tendency to increase the frequency when increasing the angular speed (parameter λ). This phenomenon occurs at lower angular speed values. At higher angular speed values frequency monotonously decrease. In addition, the influence of eccentricity on vibration frequency change is significantly less than in the fundamental mode shape, when values of λ rise to 40. All mode shapes, with the exception of (0,1), show that when $\lambda = 40$ the change in eccentricity from 0 to 0.5 results in the frequency decrease of up to 10%.

As has been mentioned earlier, in the case of asymmetric mode shapes ($n > 0$) the frequency split occurs. The frequencies determined by solving the frequency equation obtained from Eqs. (22) and (23) are represented by the continuous line, while those determined from Eq. (24) are represented by the dotted line. It can be seen that the frequency differences for the same mode shapes depend on the mode shape itself and that they are significant in the (0,1) mode shape, while being much less in the case of other mode shapes. The fact that in the (0,1) mode shape the frequency lines $(0,1)_c$ and $(0,1)_s$ intersect deserve special attention. In that case the split frequencies become equal for the certain values of the angular speed. By connecting the points with equal frequencies the line AB is obtained. It is possible that similar phenomena occur in other mode shapes as well, but they were not observed within the range of the nondimensional parameter of the angular speed (λ less than 40).

5. Mode shapes

The eccentricity of the plate rotation and its angular speed have a significant influence on the mode shape. Figs. 5–8 show the influence of the nondimensional angular speed change on mode shapes, assuming eccentricity at a value of 0.3. The mode shapes considered are (0,0), (1,0) and (0,1). The plates rotate around the *c*-axis, while *o* is the axis of symmetry of the undeformed plate.

In the case of the fundamental mode shape (0,0) the mode shape stops being axisymmetric as soon as the angular speed becomes more than zero. The deformation occurs and the “top of the hill” dislocates away from the axis of rotation due to the influence of inertial forces. A similar effect occurs in the case of increasing eccentricity at a constant angular speed, although that is not shown in the figure. Otherwise, the mode shapes are symmetrical with respect to the plane containing the axes *c* and *o*. Similar conclusions can be made in the case of the (1,0) mode shape in Fig. 6, which has a single nodal circle when the plate does not rotate. In the case of eccentric rotation the nodal circle is deformed and lengthened in the direction of inertial forces.

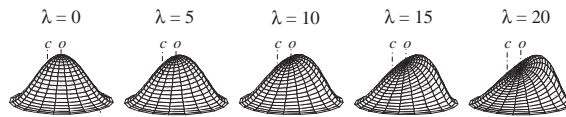


Fig 5. The effect of nondimensional angular speed variation on the mode shape (0,0) for *e* = 0.3.

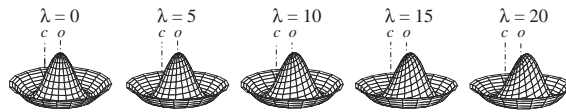


Fig. 6. The effect of nondimensional angular speed variation on the mode shape (1,0) for *e* = 0.3.

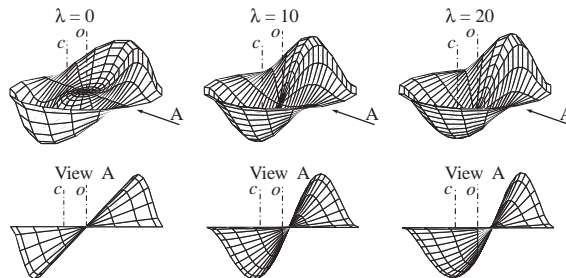


Fig. 7. The effect of nondimensional angular speed variation on the mode shape (0,1)_c for *e* = 0.3.

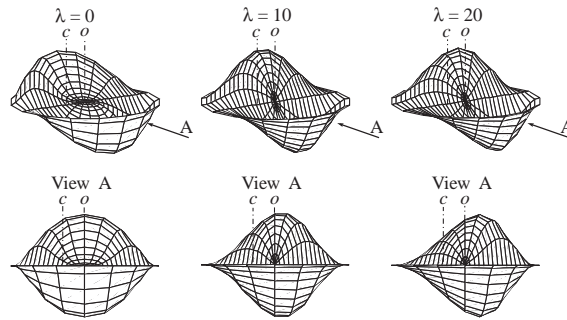


Fig. 8. The effect of nondimensional angular speed variation on the mode shape $(0,1)_s$ for $e=0.3$.

The $(0,1)$ mode shape has two variations shown in $(0,1)_c$ Fig. 7 and $(0,1)_s$ Fig. 8, because the frequency split occurs in this mode shape. The view from A direction, which is defined by the arrow shown, is given for each mode shape. The nodal diameter distorts in the $(0,1)_c$ mode shape with the plate rotation. There is a symmetry with respect to the plane containing the axes c and o in this mode shape. In the $(0,1)_s$ mode shape the nodal diameter does not distort, but remains straight. The plate deforms so that there is a symmetry with respect to the plane containing the axes c and o , and the view A is from the direction perpendicular to that plane.

6. Conclusions

The results of the present analysis of an eccentric rotating circular plate may be summarized as follows:

1. The influence of eccentricity and angular speed on transverse vibration frequencies is especially large in the case of $(0,0)$ and $(0,1)$ mode shapes. With the higher mode shapes the influence of eccentricity on frequencies is substantially less for the values of λ considered.
2. There are two frequency equations which result in the frequency split in asymmetric ($n \neq 0$) mode shapes. The difference between the two frequencies is significant in the $(0,1)$ mode shape.
3. Eccentricity and rotation can result in the loss of stability of the plate. Critical angular speed decreases with eccentricity increase.
4. The mode shapes deform additionally due to the influence of eccentricity and inertial force. The tendency of moving away the “top of the hill” from the axis of rotation can be observed in cases of the fundamental $(0,0)$ and the $(1,0)$ mode shapes.

Acknowledgements

This research was supported by the Ministry of Science, Technologies and Development of Republic of Serbia, project no. 1402.

References

- [1] T.P. Mitchell, W.E. Warren, The stresses in a thin circular disk rotating about an eccentric circular rigid insert, *International Journal of Mechanical Sciences* 5 (1963) 137–148.
- [2] A.I. Lurie, *Theory of Elasticity*, Nauka, Moscow, 1970 (in Russian).
- [3] H.B. Khurasia, S. Rewtant, Vibration analysis of circular plates with hole, *Journal of Applied Mechanics* 45 (1978) 215–217.
- [4] L. Cheng, Y.Y. Li, L.H. Yam, Vibration analysis of annular-like plates, *Journal of Sound and Vibration* 262 (2003) 1171–1189.
- [5] R.G. Parker, C.D. Mote, Exact perturbation for the vibration of almost annular or circular plates, *Journal of Vibration and Acoustics* 118 (1996) 436–455.
- [6] J. Chung, J.W. Heo, C.S. Han, Natural frequencies of a spinning disk misaligned with the axis of rotation, *Journal of Sound and Vibration* 260 (2003) 763–775.
- [7] J.W. Heo, J. Chung, K. Choi, Dynamic time responses of a flexible spinning disk misaligned with the axis of rotation, *Journal of Sound and Vibration* 262 (2003) 25–44.
- [8] A.W. Leissa, *Vibration of Plates (NASA SP 160)*, US Government Printing Office, Washington DC, 1969.
- [9] R. Margetic, Vibration and stability of rotating plates with elastic edge supports, *Journal of Sound and Vibration* 210 (1998) 291–294.